Supporting Information

Electrical Control of Shape in Voxelated Liquid Crystalline Polymer Nanocomposites

Tyler Guin,[†‡] *Benjamin A. Kowalski,*[†‡] *Rahul Rao,*[†ⱡ] *Anesia D. Auguste,*[†] *Christopher A. Grabowski,*[†§] *Pamela F. Lloyd,*[†§] *Vincent P. Tondiglia,*[†‡] *Benji Maruyama,*[†] *Richard A. Vaia,*[†] *Timothy J. White*[†]*

[†] Air Force Research Laboratory, Materials and Manufacturing Directorate, 3005 Hobson Way, Wright-Patterson AFB, Ohio, 45433-7750, USA

[‡] Azimuth Corporation, 4027 Colonel Glenn Highway, Beavercreek, Ohio 45431, USA

[§] UES, Inc., 4401 Dayton Xenia Rd, Beavercreek, Ohio 45432, USA

Contact: timothy.white.24@us.af.mil

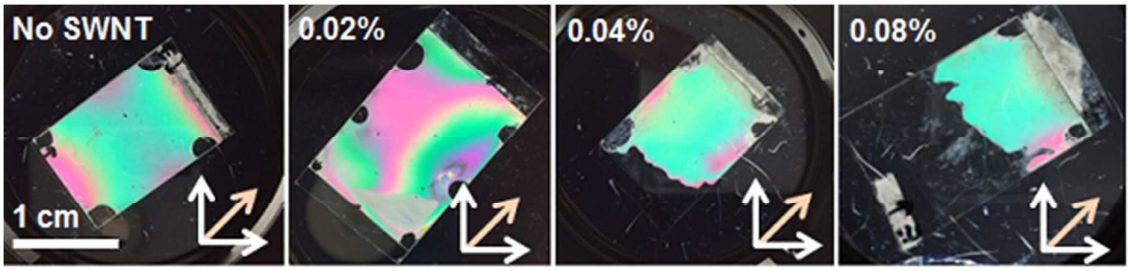

Figure S1. Cross-polarized images of 8 µm thick, homogeneous planar LC cells filled with SWNT-LCEs with varying concentrations of SWNT. The viscosity of the mixture increases with increases SWNT loading, preventing filling of the entire cell at 100°C.

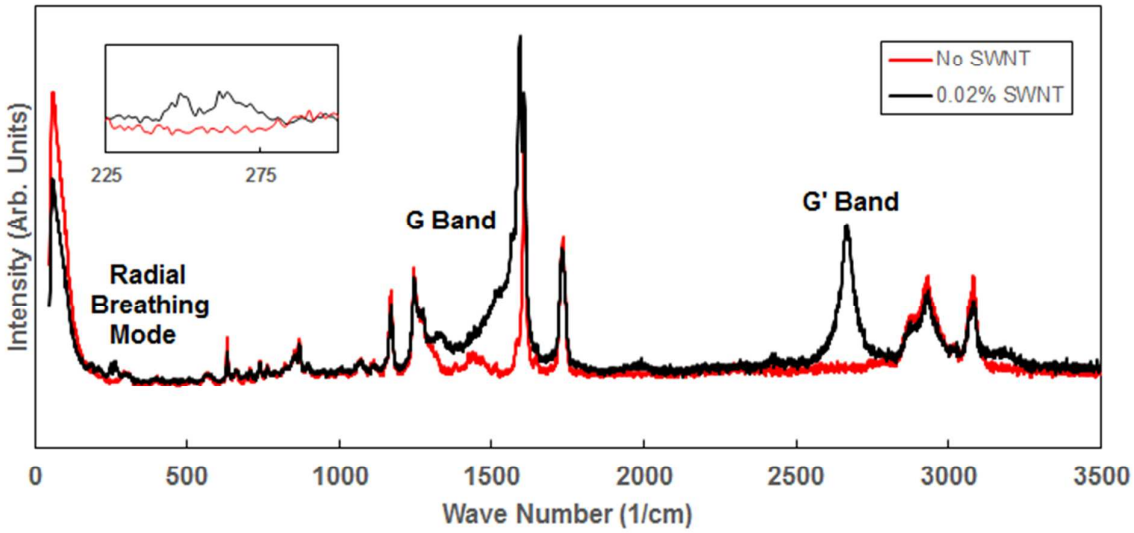

Figure S2. Raman spectra of 15 µm thick, homogeneous planar SWNT-LCEs with and without SWNT. The G' band was chosen to represent the SWNT as it is removed from any LCE peak. Inset is a close-up view of the radial breathing modes.

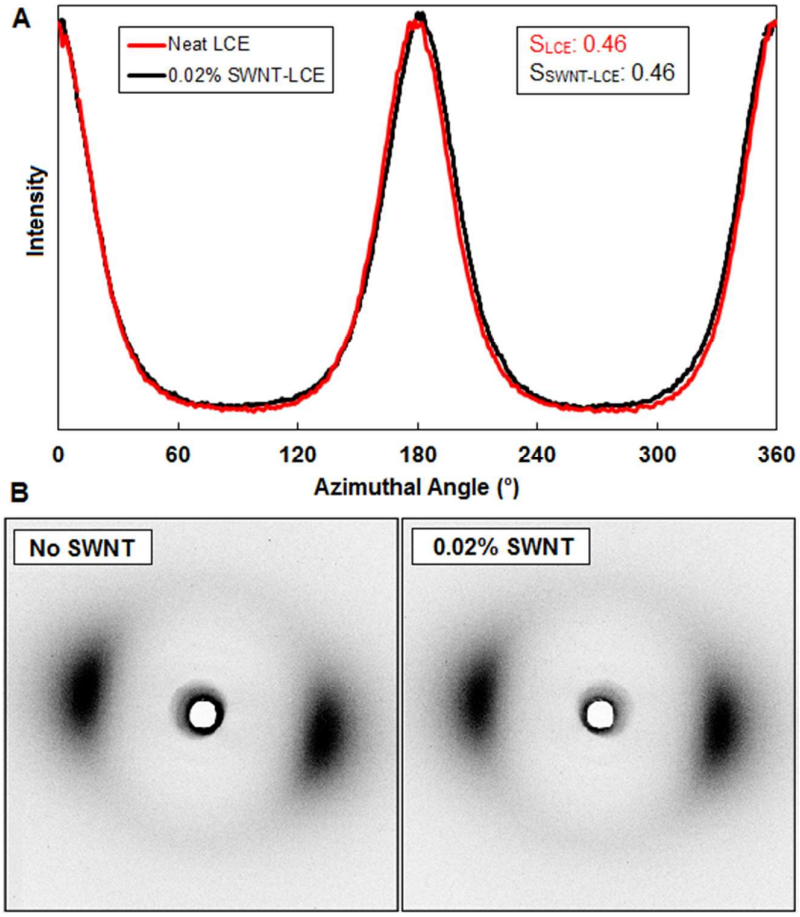

Figure S3. (a) X-ray scattering intensity at the 19.4° 2-theta peak as a function of azimuthal angle, and (b) X-ray scattering profile of a 15 µm thick homogeneous planar SWNT-LCE with and without SWNT. This profile is indicative of a well-aligned nematic system.

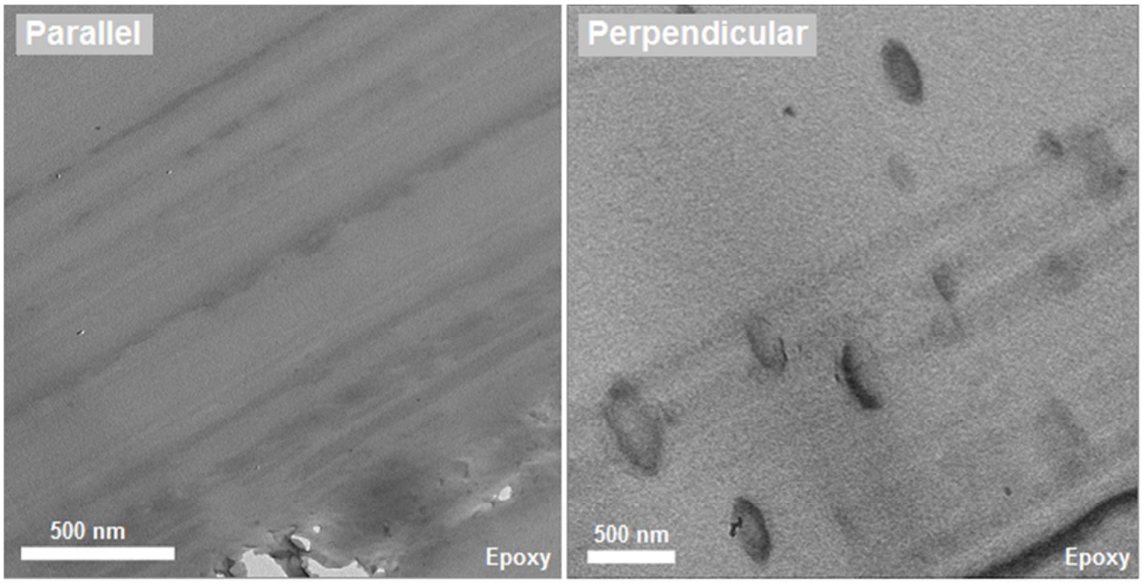

Figure S4. Transmission electron micrographs of 0.02% SWNT-LCE films cut parallel or perpendicular to the LCE / SWNT orientation direction.

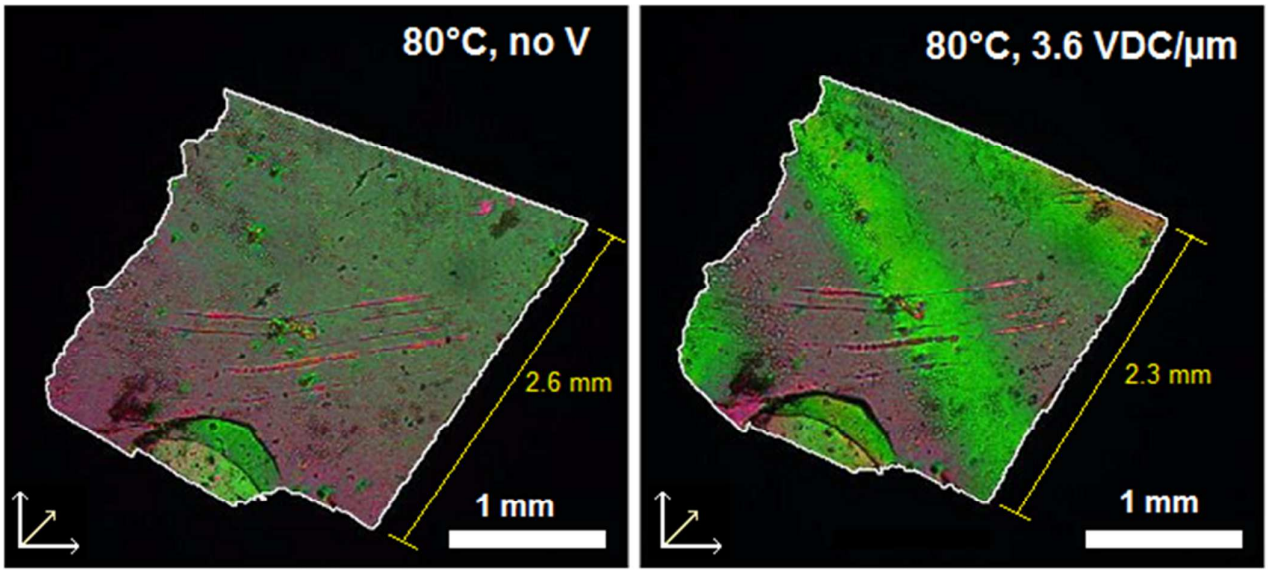

Figure S5. 15 µm thick, homogeneous planar 0.02% SWNT-LCE film floating in silicone oil between ITO plates spaced 100 µm apart at 80°C (left). Upon exposure to a 3.6 VDC/µm electric field, the film contracts and bends along the director (right).

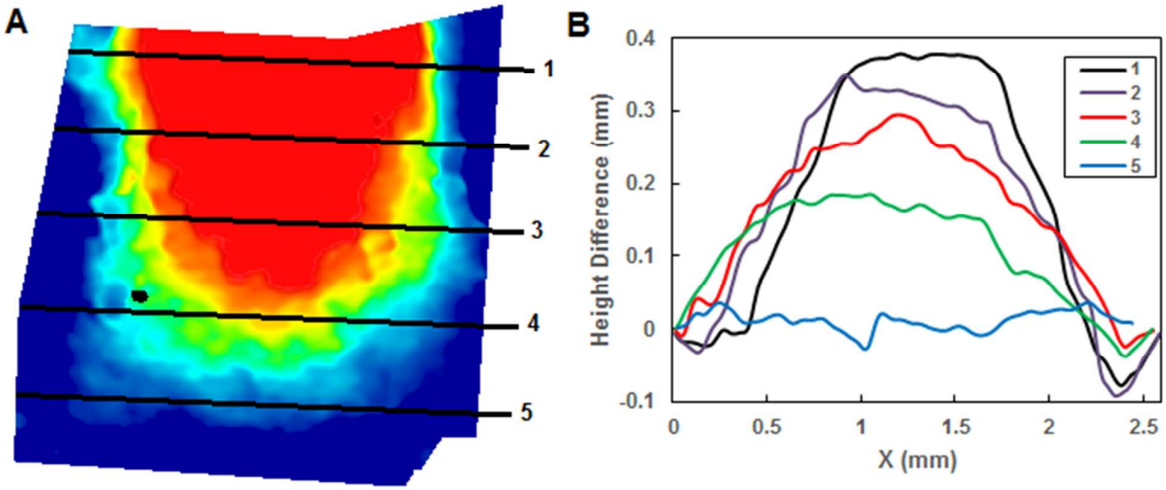

Figure S6. (a) Height map difference between a 0.02% SWNT-LCE film, patterned into a +1 topological defect, before and after a 1.2 VDC/µm field is applied at 90°C, and (b) traces across the height map. The height maps indicates significant localized shape change throughout the film during electrical activation.

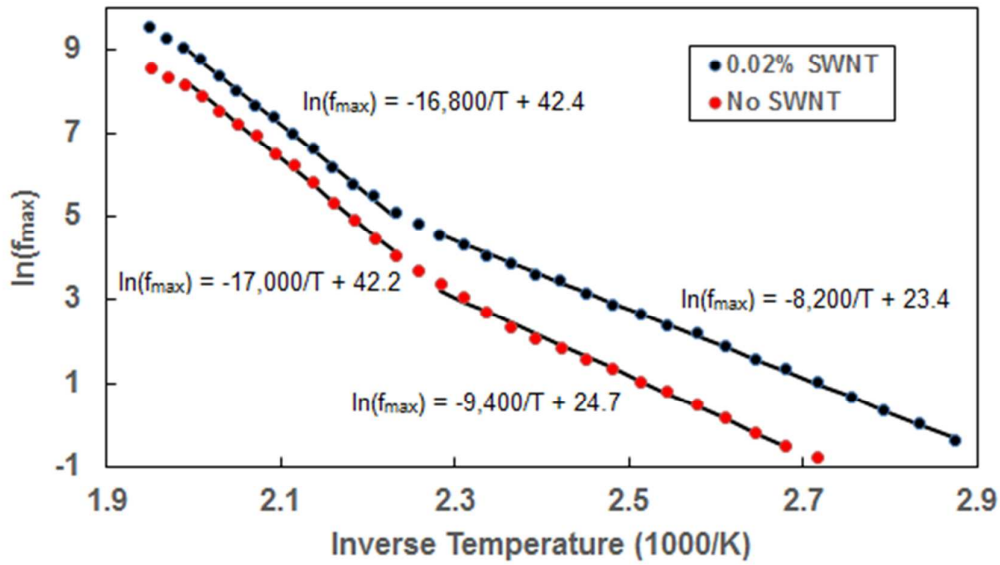

Figure S7. Relaxation peak from dielectric relaxation spectroscopy as a function of inverse temperature for samples with and without SWNT. Fitted curves are obtained for before and after the para-nematic transition temperature, and the slope is directly proportional to the dipole rotational activation energy. E_a (No SWNT, low T) = 78.1 kJ/mol; E_a (No SWNT, high T) = 141.7 kJ/mol; E_a (No SWNT, low T) = 68.6 kJ/mol; E_a (No SWNT, low T) = 139.5 kJ/mol.

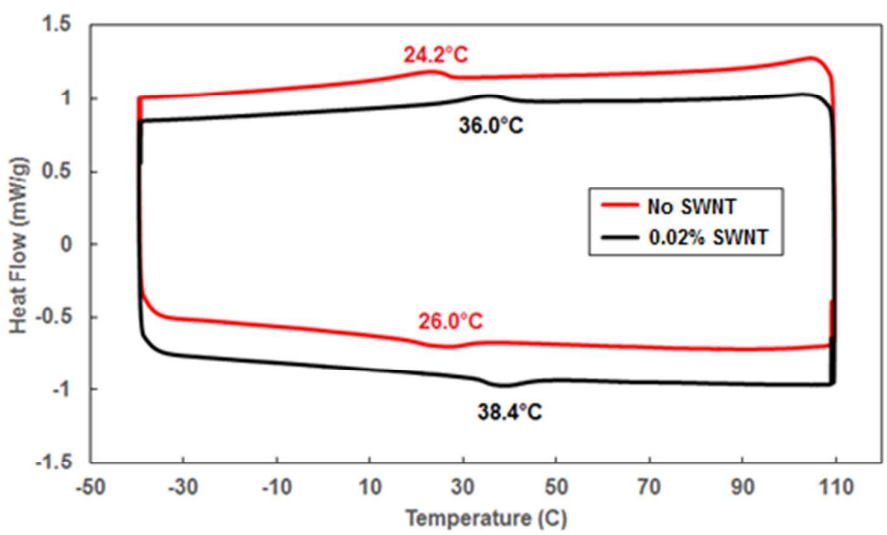

Figure S8. DSC traces of monomer mixtures with and without SWNT. Traces shown are the second heating and cooling. No crystallization peak is apparent down to -40°C, and the nematic transition is very broad.